Accepted Manuscript

The influence of ageing on the stabilisation of interfacial $(Cu,Ni)_6(Sn,Zn)_5$ and $(Cu,Au,Ni)_6Sn_5$ intermetallics in Pb-free Ball Grid Array (BGA) solder joints

Guang Zeng, Stuart D. McDonald, Dekui Mu, Yasuko Terada, Hideyuki Yasuda, Qinfen Gu, M.A.A. Mohd Salleh, Kazuhiro Nogita

PII: S0925-8388(16)31624-3

DOI: 10.1016/j.jallcom.2016.05.263

Reference: JALCOM 37783

To appear in: *Journal of Alloys and Compounds*

Received Date: 18 January 2016

Revised Date: 22 May 2016

Accepted Date: 23 May 2016

Please cite this article as: G. Zeng, S.D. McDonald, D. Mu, Y. Terada, H. Yasuda, Q. Gu, M.A.A.M. Salleh, K. Nogita, The influence of ageing on the stabilisation of interfacial $(Cu,Ni)_6(Sn,Zn)_5$ and $(Cu,Au,Ni)_6Sn_5$ intermetallics in Pb-free Ball Grid Array (BGA) solder joints, *Journal of Alloys and Compounds* (2016), doi: 10.1016/j.jallcom.2016.05.263.

The influence of ageing on the stabilisation of interfacial $(Cu,Ni)_6(Sn,Zn)_5$ and $(Cu,Au,Ni)_6Sn_5$ intermetallics in Pb-free Ball Grid Array (BGA) solder joints

Guang Zeng[1], Stuart D. McDonald[1], Dekui Mu[2,3], Yasuko Terada[4], Hideyuki Yasuda[5], Qinfen Gu[6], M.A.A.Mohd Salleh[1,7], and Kazuhiro Nogita[1*]

[1] Nihon Superior Centre for the Manufacture of Electronic Materials (NS CMEM), School of Mechanical and Mining Engineering, The University of Queensland, St Lucia, QLD 4072, Australia;

[2] Nihon Superior Co. Ltd., Suita-City, Osaka 564-0063, Japan;

[3] Institute of Manufacturing Engineering, Huaqiao University, Xiamen 361021, China;

[4] The Japan Synchrotron Radiation Research Institute, Mikazuki-cho, Hyogo 679-5198, Japan;

[5] Department of Materials Science and Engineering, Kyoto University, Sakyo-ku, Kyoto 606-8501, Japan;

[6]. Powder Diffraction Beamline, The Australian Synchrotron, Clayton, VIC 3168, Australia;

[7]. Centre of Excellence Geopolymer and Green Technology, School of Materials Engineering, Universiti Malaysia Perlis (UniMAP), Taman Muhibbah 02600, Jejawi, Arau, Perlis, Malaysia.

*Corresponding author, tel, +61-7-3365-3919, fax, +61-7-3365-4799, e-mail, k.nogita@uq.edu.au

Abstract

Formation/growth behaviour, phase stability, and mechanical properties of interfacial Cu_6Sn_5 intermetallics influenced by micro-alloying in Pb-free solder joints, are of ongoing interest as this phase is crucial to the service reliability of solder joints. Our recent work has demonstrated that, after reflow, the homogeneously located micro-alloying elements of both Ni and Zn in interfacial $(Cu,Ni)_6(Sn,Zn)_5$ act to increase phase stability and prevent the undesirable polymorphic phase transformation of Cu_6Sn_5. This paper further investigates the influence of ageing on the phase stability of interfacial intermetallics containing Ni, Zn and Au. Phase transformations of hexagonal to monoclinic Cu_6Sn_5 driven by ageing, was suppressed by alloying Ni/Zn/Au, resulting in improvements in phase stability. The findings help to further understand the reliability of interfacial structures in micro-alloyed Pb-free solder joints.

Keywords: Solder, Synchrotron radiation; X-ray diffraction; Intermetallics; Phase transitions

1. Introduction

"Micro-alloying", i.e., the creation and development of new alloys through minor/trace element additions [1], can greatly influence the solidification microstructure and interfacial reactions in Pb-free solder joints [1-5]. Ni, Zn and Au are candidates for the micro-alloying of Sn-rich solder alloys. The formation and growth of the technically important Cu_6Sn_5 intermetallic phase (in both bulk solder and at the interface of solder joints) are influenced by these trace element additions[2, 4, 6]. For instance, $(Cu,Ni)_6Sn_5$, $Cu_6(Sn,Zn)_5$ and $(Cu,Au)_6Sn_5$ intermetallics form at the solder/substrate interface when Cu or Sn atoms in Cu_6Sn_5 are replaced with microalloying elements [7]. Consequently the size, morphology, growth orientation, growth kinetics and stability of interfacial intermetallics can vary depending on the amount of alloying elements. Ni is found to be one of the most effective alloying elements and has been proven to significantly improve the microstructure and properties of Sn-0.7wt.%Cu solders [7-15]. With the addition of trace amounts of Ni (0.05wt.%), Sn-0.7wt%Cu solder shows a refined eutectic structure after solidifying at cooling rates from 2℃/min to 30℃/min [1, 16, 17]. The Ni also acts to increase the fluidity of Sn-0.7wt%Cu during solidification[18]. During soldering processes Ni also concentrates within the interfacial intermetallic layer to form the $(Cu,Ni)_6Sn_5$ phase which is adjacent to the Cu substrate [1, 19]. Meanwhile, Ni suppresses interfacial Cu_3Sn growth during both reflow and ageing processes [20, 21]. During interfacial reactions between molten Sn-0.7Cu-0.05Ni and Cu substrates, Ni additions promote the nucleation of a larger amount of small Cu_6Sn_5 compared to Ni-free Sn-0.7Cu . The growth orientation of interfacial Cu_6Sn_5 is also altered by Ni additions [22] and the impact strength is improved [23].

Zn significantly reduces the nucleation undercooling of β-Sn in Sn based Pb-free solder alloys [24]. Cu-Zn intermetallics precipitates appear as dispersed particles between the primary β-Sn and eutectic regions in Sn-0.7Cu-0.15Zn alloys [25]. The formation of precipitated Cu-Zn intermetallics can be correlated with an enhancement of tensile strength and hardness. Au is another common element used in Pb-free solder systems in both the metallization of substrates and the microalloying of solder alloys. Huh et al.[26] found that the width of inter-dendritic eutectic areas decreased as 1.0wt.% Au was added to Sn-0.7Cu, and $AuSn_4$ formed at the region of the inter-dendritic eutectic [26]. Recently, Balyakov et al. [27] discovered that $AuSn_4$ was a relatively ineffective catalyst for βSn nucleation compared to $NiSn_4$, $PdSn_4$ and $PtSn_4$.

Interestingly, in terms of the crystallographic stability of Cu_6Sn_5, there are several types of polymorphs [28-32], as detailed in Table 1 [33]. Ni stabilises the high-temperature hexagonal ($P6_3/mmc$) polymorph η-Cu_6Sn_5 in Pb-free solder alloys/joints over the range of -80 to 240℃ [8, 13]. The solubility of Ni in the Cu_6Sn_5 phase can be as large as 17 at.% by replacing Cu atoms [8] (at room temperature), while the minimum Ni concentration in $(Cu,Ni)_6Sn_5$ required for preventing a polymorphic phase transformation can be as low as 1 at.% [13]. Furthermore, in our previous studies [34], it was found that $Cu_6(Sn,Zn)_5$, $(Cu,Au)_6Sn_5$ and $Cu_6(Sn,In)_5$ (with In ≥7.1 at.%) remained stable as the high temperature hexagonal variant of Cu_6Sn_5 over the range of -80 to 240℃, successfully suppr essing the polymorphic phase transformation. Our recent findings [1] further showed that concurrent additions of Ni and Zn in Sn-0.7Cu significantly refined the microstructure of the bulk solder alloy, and also lead to a more continuous, refined and stable interfacial

$(Cu,Ni)_6(Sn,Zn)_5$ layer. Concurrent Ni/Zn alloying minimises the thermal expansion mismatch between interfacial Cu_6Sn_5 and Cu.

When reflowed solder joints are subjected to subsequent ageing, diffusion of Ni within Cu_6Sn_5 is found to be very limited in Sn-0.7Cu-0.05Ni/Cu Ball Grid Array (BGA) solder joints [20]. As a result the phase stability of Cu_6Sn_5 is slightly comprised by Ni segregation, resulting in η' phase growth during 150℃ ageing. Meanwhile, as mentioned above, after reflow, the combination of Ni and Zn are complementary in refining the microstructure and stabilising interfacial $(Cu,Ni)_6(Sn,Zn)_5$ intermetallics [1]. However, the degree to which these benefits brought about by Ni/ Zn micro-alloying are sustained with ageing are unclear, despite this being a critical issue for the long-term reliability of solder joints. With respect to Au, although it is known that Au completely stabilised η-Cu_6Sn_5 in powder form [34, 35], its impact on the interfacial $(Cu,Au)_6Sn_5$ in both the as-reflowed and aged condition remains unexplored, including the distribution of this element within Cu_6Sn_5.

In this study, based on our previous findings [1, 20, 25, 34], we aimed to further explore the effects of ageing on the distribution of the trace elements Ni, Zn and Au in micro-alloyed Sn-0.7Cu/Cu BGA joints, and the phase stability of the $(Cu,Ni)_6(Sn,Zn)_5$ or $(Cu,Au,Ni)_6Sn_5$ intermetallic layer with respects to crystal structure, by means of synchrotron glancing angle X-ray diffraction (XRD) and synchrotron micro X-ray fluorescence analysis (XRF). The effect of alloying with Au on the thermal expansion behavior of interfacial Cu_6Sn_5 intermetallics was also investigated for the first time. This study is an important progression of our previous findings [1, 20], and investigates the influence of ageing on the stabilisation effects.

2. Materials and methods

Samples and experimental setup are shown in Fig.1(a-f). Solder joints (in wt.%) were prepared by a reflow process and dipping method, respectively. Ball Grid Aarry (BGA)s were manufactured with individual balls with a diameter in the range of 500 to 600 μm. The test samples were reflowed on organic solderability preservative (OSP)-finished 30 μm thick Cu plating on FR-4 printed circuit boards (PCBs) by contact bonding. RM-5 flux (Nihon Superior Co., Ltd., Japan) was used for reflow soldering. These samples experienced two reflows (a peak temperature of 250℃ and half of the samples were also subjected to ageing at 150℃ for 500h and 1500h. After soldering and subsequent ageing, samples were embedded in resin and polished to a thickness of ~100 μm, along the cross-sectional direction to the solder interface, using conventional grinding and polishing techniques for sample preparation. The thinned BGA sample is displayed in Fig.1(b). Dipping samples were prepared by dipping the Cu plates (C1220P) of 10 mm×30 mm×0.3 mm with Inorganic Acid Water Soluble Flux (Nihon Superior Co., Ltd., Japan) into the molten solder in a solder bath at 270℃. Selected samples were etched before and after ageing at 150℃ in a solution of ortho-nitrophenol (35 g) and NaOH (50 g) in 1 L of water at 80℃ to completely remove the Sn-rich part s of solder alloys, as show in Fig.1(e-f). Samples were observed using a JEOL7001F Scanning Electron Microscope (SEM) under the backscatter mode with an acceleration voltage of 20kV.

Micro-XRF experiments were carried out at beamline BL37XU of the SPring-8 synchrotron with experimental settings as illustrated in Fig.1a and 1d and also identical to those detailed and Ref.[36]. The measurements were conducted at an X-ray energy intensity of 12keV. The data was processed and analysed using Igor

6.32A software. The penetration depth of the X-ray to the specimen is a critical value to determine which part of the specimen was measured. Diffraction data were obtained from the prepared dipped samples, in flat-plate asymmetric reflection geometry at the powder diffraction beamline of the Australian Synchrotron [37, 38]. An X-ray energy of 15keV was used. The Wavelength (0.8266Å) and 2θ zero-error were determined from a standard 0.3 mm capillary of a LaB_6/Si mixture using transmission geometry. The angle between the X-ray beam and the sample surface was fixed at 5°, as shown in Fig.1d. In this case, the practical depth of analysis for the Cu_6Sn_5 layer with an X-ray beam is ~2μm [39]. Indexing and whole pattern Le-Bail refinement of XRD patterns was conducted using TOPAS 4.2 software. A Fundamental parameter (FP) approach was employed in TOPAS to perform whole-pattern profile fitting of the diffraction data collected in parallel-beam flat-plate asymmetric reflection [38], as shown in Fig.1d (experiment setup) and Fig.2 (whole pattern fitting).

3. Results and discussion

3.1 Morphology of $(Cu,Ni)_6Sn_5$, $Cu_6(Sn,Zn)_5$, $(Cu,Ni)_6(Sn,Zn)_5$ and $(Cu,Ni,Au)_6Sn_5$

Fig.3 and 4 show that the back-scattered SEM images of the BGA solder joints subjected to reflow and subsequent ageing at 150^{o}C for 500h. Coarsening of the Cu_6Sn_5 intermetallic is more distinguishable in Sn-0.7Cu-0.4Zn-0.03Ni/Cu compared to Sn-0.7Cu-0.06Au-0.05Ni/Cu. It is also noted that the IMC particles accumulated in the near outer surface area of Sn-0.7Cu-0.4Zn-0.03Ni/Cu BGA balls as shown in Fig.3 (c) and (d). This is likely due to the settling of some Cu_6Sn_5 intermetallic particles that have not been completely melted by the reflow process under the

influence of gravity. An alternative or complimentary mechanism may be the heterogeneous nucleation and growth of Cu_6Sn_5[6], possibly catalysed by the surface oxidation layer of the solder ball or impurity elements. Also in Sn-0.7Cu-0.06Au-0.05Ni/Cu BGA joints, surface accumulation of Cu_6Sn_5 is not so obvious, possibily due to the differences in the solidification path compared to Sn-0.7Cu-0.4Zn-0.05Ni/Cu. Fig.5 reveals the morphology of the interfacial layer of Sn-0.7Cu BGA solder joints varied with micro-alloying Ni/Zn/Au elements. Sn-0.7Cu-0.4Zn-0.03Ni, Sn-0.7Cu-0.06Au and Sn-0.7Cu-0.06Au-0.05Ni are compared to compositions with Ni and Zn additions studied in previous works (Sn-0.7Cu, Sn-0.7Cu-0.05Ni, Sn-0.7Cu-0.15Zn and Sn-0.7Cu-0.06Zn-0.05Ni) [1, 20]. The major differences in these samples are the presence, morphology and thickness of Cu_3Sn between the Cu_6Sn_5 and Cu substrates.

Interfacial IMC growth is dramatically different in liquid-solid reactions compared with solid-solid reactions during ageing, in terms of diffusion species, alloying element distribution and interfacial phase growth kinetics. It is generally considered that Cu_6Sn_5 approximately follows $t^{1/3}$ kinetics via Ostwald ripening in liquid/solid interfacial reactions, whilst diffusion controlled kinetics generally follow a parabolic law of $t^{1/2}$ in solid-solid reactions[17, 40].Gong et al. [41] confirmed that the $Cu_6Sn_5/Cu_3Sn/Cu$ sandwich structure formed at the interface during the early stage of Cu/molten solder interfacial reactions and this structure remained throughout the whole reflow process. The growth morphology and kinetics of interfacial Cu_6Sn_5 are basically determined by nucleation of Cu_6Sn_5 and dissolution of Cu from the substrate [42]. The migration of the Cu_6Sn_5/Cu_3Sn interface is controlled by the supply of Cu and Sn atoms from both sides [41]. When the flux of Cu supplied from

the substrate is comparable with Sn contributed from the solder side during solid-state ageing [41], the Cu_6Sn_5 and Cu_3Sn layers have similar thicknesses, as shown in Sn-0.7Cu/Cu of Fig.5. Alloying elements are found to significantly influence the Cu_6Sn/Cu_3Sn thickness ratio [19, 43-45]. In our previous study we have identified that interfacial Cu_3Sn can be efficiently suppressed in Sn-0.7Cu-0.06Zn-0.05Ni [1]. Kao et al. [46] determined the threshold value for effectively suppressing Cu_3Sn in Sn-2.5Ag-0.8Cu/Cu was 0.01 wt.%Ni at a minimum, when subjected to 2000h ageing. In the present study (Fig.5), Zn as an individual addition suppressed the growth of Cu_3Sn similar to Ni when the content of Zn reached 0.4 wt.%. Cu_3Sn could hardly be observed in the Sn-0.7Cu-0.4Zn-0.03Ni/Cu alloy after 500h ageing, with the combined influence of both 0.4wt.%Zn and 0.05 wt.%Ni from the alloys. In contrast, the Cu_3Sn layer was clearly present in Au containing samples of Sn-0.7Cu-0.06Au/Cu and Sn-0.7Cu-0.06Au-0.05Ni/Cu. It is concluded that Au is not as effective as Ni/Zn in terms of suppressing the growth of Cu_3Sn in the interfacial intermetallic layer of the Sn-0.7Cu/Cu system. The following sections consider the mechanisms of Cu_3Sn suppression as they relate to trace element additions using XRD focusing on the interfacial region.

3.2 Trace element analysis of Zn, Au and Ni in interfacial intermetallics

A focus of this study was to understand how ageing influences the Au/Zn/Ni distribution in interfacial Cu_6Sn_5 and also the phase stability of Cu_6Sn_5 . XRF mapping was performed by synchrotron radiation to achieve high-resolution (50 nm at minimum) elemental mapping of the interfacial intermetallics. Due to the possibility of different characteristic X-ray peaks overlapping, corresponding point analysis (Point A-I in Fig.6-8) was conducted to ensure the accuracy of mapping.

Deconvolution of spectrums for selected elements was performed by extracting the net peak intensity/width with fitting Gaussians to peaks (Point B in Fig.6, the detailed procedure is documented in [1]). The processed mapping results in Fig.6, especially Ni/(Cu+Ni) and Zn/(Cu+Zn), confirm that Ni and Zn are both relatively homogenously distributed within Cu_6Sn_5 in as-reflowed Sn-0.7Cu-0.06Zn-0.05Ni/Cu BGA samples. This was consistent with the results in our previous work [1] in the form of dipped samples of identical composition. The same conclusion can be made that the effect of Ni was slightly stronger than Zn at a similar level of addition (0.06 wt.% Zn versus 0.05 wt.% Ni addition). It is also noted that $(Cu,Ni)_6(Sn,Zn)_5$ intermetallic particles formed within the solder matrix near the intermetallic layer after reflow.

In the case of Au/Ni concurrent additions (Sn-0.7Cu-0.06Au-0.05Ni/Cu), as displayed in Fig.7, Au and Ni both concentrated in the interfacial Cu_6Sn_5 and also the intermetallics in the near-interface region of the solder matrix. After ageing for 500h (Fig.8), Cu_3Sn was present between the $(Cu,Au,Ni)_6Sn_5$ and Cu layers, as revealed by both SEM imaging and also micro-XRF mapping. The Cu elemental mapping is plotted twice in Fig.8 with a different colorscale to clearly show the two distinct intermetallic layers of Cu_6Sn_5 and Cu_3Sn, with the help of an intensity mask (intensities lower than 100 counts and higher than 2,200 counts are colored in grey). In Sn-0.7Cu-0.06Au-0.05Ni after 500h ageing, Ni also segregated but was mainly located in the Cu_3Sn, in contrast to Sn-0.7Cu-0.05Ni/Cu [20] and Sn-0.7Cu-0.06Zn-0.05Ni [1]. Ni was concentrated within Cu_3Sn and only a small amount of Ni was detected on the top of the Cu_6Sn_5 phase. Obviously, the Ni concentration in Cu_3Sn was higher than that in the adjacent Cu_6Sn_5 layer, which was consistent with previous studies by other researchers. It has been found that Ni was able to dissolve

in Cu_3Sn by replacing Cu atoms during ageing [47, 48]. Au was still relatively homogeneously distributed in Cu_6Sn_5 and this was similar to the behavior of Zn in interfacial $(Cu,Ni)_6(Sn,Zn)_5$ phase [1], however, no obvious solubility of Au in Cu_3Sn was found.

On the inter-diffusion of the solder/Cu system, there are three interfaces with four potential interfacial reactions, listed as Reaction 1 to 4 [7, 49-52]. Minor Ni and Au alloying elements are unlikely to form any other phases at the interfaces but would dissolve into Cu_3Sn or Cu_6Sn_5.

Interface 1 $3Cu+Sn \rightarrow Cu_3Sn$ (1)

Interface 2 $2Cu_3Sn+3Sn \rightarrow Cu_6Sn_5$ (2)

$Cu_6Sn_5+9Cu \rightarrow 5Cu_3Sn$ (3)

Interface 3 $5Sn+6Cu \rightarrow Cu_6Sn_5$ (4)

As aforementioned, the migration of the Cu_6Sn_5/Cu_3Sn interface, i.e. either Reaction (2) or Reaction (3) is dominant and is controlled by the diffusion of Cu and Sn atoms from both sides. It is well documented that Ni dissolving into Cu_6Sn_5 causes a change of diffusion driving forces of Cu and Sn through interfacial Cu_3Sn and Cu_6Sn_5[53, 54]. As a result, this influences the diffusion fluxes and subsequently the growth of phases. According to the thermodynamic assessment of the Sn-Cu-Ni ternary system by Vuorinen et al.[55], the diffusion driving fluxes of both Sn and Cu were increased with the content of Ni in $(Cu,Ni)_6Sn_5$. However, increase of Ni content in $(Cu,Ni)_3Sn$ decreased the diffusion fluxes of Sn and Cu in $(Cu,Ni)_3Sn$[55]. Therefore, $(Cu,Ni)_6Sn_5$ is more favourable and became the dominant phase, i.e. Reaction (2) takes precedence over Reaction (3)and Cu_3Sn growth is suppressed

[51].

On the other hand, Ni content varies along the interfacial intermetallics due to the local equilibrium requirements combining with mass-balance rules[53]. As explained in Ref.[53], based on the Sn-Cu-Ni phase diagram, in the Cu_6Sn_5/Cu_3Sn two phase regions, at local equilibrium the Ni content in $(Cu,Ni)_3Sn$ is expected to be higher than that in $(Cu,Ni)_6Sn_5$. Thermodynamically the partitioning of Ni should occur between $(Cu,Ni)_6Sn_5$ and $(Cu,Ni)_3Sn$. The Ni content should decrease towards the $(Cu,Ni)_3Sn$/$(Cu,Ni)_6Sn_5$ interface[53]. Moreover, the interdiffusion coefficient of the Cu_6Sn_5 phase at 150℃ is estimated to be 2.5×10^{-13} to 3.8×10^{-12} cm^2/s [40, 56, 57], whilst Ni interdiffusion coefficients in the Cu_6Sn_5 are $< 8.3 \times 10^{-15}$ cm^2/s at 150℃[58].

In contrast, with Sn-0.7Cu-0.06Au-0.05Ni/Cu, Ni was mainly traced in the Cu_3Sn phase strongly indicating that Ni hardly diffused through Cu_6Sn_5/Cu_3Sn, and Reaction (3) was dominant so the growth of Cu_3Sn is distinct after 500h ageing. Therefore, the Au addition was ineffective in suppressing Cu_3Sn growth separately, and harmful to the Ni suppression effect with Ni/Au concurrent additions. This differs from the minimal amounts of Cu_3Sn phase that existed along with $(Cu,Ni)_6(Sn,Zn)_5$ and Ni segregation within $(Cu,Ni)_6(Sn,Zn)_5$ [1]. It was also noted that the solubility of Au in $(Cu,Au)_3Sn$ was slightly lower than that in $(Cu,Au)_6Sn_5$ and the apparent Au distribution is richer in both the interfacial Cu_6Sn_5 layer and the Cu_6Sn_5 particles located in the solder matrix (Fig.8). This result is consistent with the findings in Ref.[59-61], where the Au solubility in Cu_6Sn_5 was apparently higher because the Cu diffusion coefficient was approximately 1 order of magnitude larger than the diffusion coefficient of Au in $(Cu,Au)_6Sn_5$[59]. In this case, Au diffuses much faster than Ni in

Cu_6Sn_5, and furthermore, Au does not increase the diffusion flux of Cu and Sn in Cu_6Sn_5 and decrease those in Cu_3Sn. Therefore, compared to the significant effects of Ni and Zn, Au does it appears that there is no obvious influence in the thickness ratio of Cu_6Sn_5/Cu_3Sn. Moreover, Au has a poisoning effect on the Ni suppression of Cu_3Sn in Sn-0.7Cu-0.06Au-0.05Ni/Cu as both $(Cu,Au)_6Sn_5$ and $(Cu,Au)_3Sn$ are present after 500h ageing. This differs from the domination of $(Cu,Ni)_6Sn_5$ over Cu_3Sn in Ni/Zn containing solder joints.

3.3 Influence of ageing on the phase stability of interfacial $(Cu,Ni)_6Sn_5$, $Cu_6(Sn,Zn)_5$, $(Cu,Ni)_6(Sn,Zn)_5$ and $(Cu,Ni,Au)_6Sn_5$

The polymorphic phase transformations of Cu_6Sn_5 are suppressed by alloying elements (Ni, Zn, Au, In and Pd) or fast cooling rates [1, 20, 34, 35, 62, 63]. Using high-resolution synchrotron XRD, it has been found that the monoclinic Cu_6Sn_5 phase formed during the normal cooling period of reflow, as shown in Ref. [1] and Sn-0.7Cu/Cu at 0h in Fig.9. However, in the as-soldered condition, a relatively homogeneous distribution of Ni/Zn in Cu_6Sn_5 (Fig.6) could be beneficial to phase stability and hence prevent polymorphic phase transformations of Cu_6Sn_5 [1]. Based on our previous findings in the powder form of $(Cu,Au)_6Sn_5$ [35], it can be expected that Au suppresses the polymorphic phase transformation of interfacial Cu_6Sn_5 intermetallics similar to Ni/Zn. Ni and Zn are relatively homogeneously distributed within the interfacial Cu_6Sn_5, however, the concentration of Ni in Cu_6Sn_5 was larger than that of Zn. The presence of Ni and Zn within the interfacial Cu_6Sn_5 resulted in a more stable interfacial layer, inhibiting the polymorphic phase transformation of Cu_6Sn_5. Consequently, the thermal expansion mismatch between interfacial Cu_6Sn_5 and the Cu substrate was further minimised. In contrast to the as-reflowed

state, ageing may cause two changes to the phase stability, including segregation of the alloying elements within Cu_6Sn_5 and also acceleration of the hexagonal-monoclinic phase transformation in interfacial Cu_6Sn_5, based on the temperature-time-transformation (TTT) diagram of Cu_6Sn_5 [29, 63]. In Sn-0.7Cu-0.05Ni/Cu, the phase stability of interfacial $(Cu,Ni)_6Sn_5$ is compromised by the limited solid-state diffusion of Ni in Cu_6Sn_5 and the inhomogeneous Ni distribution during ageing [20]. Therefore, there is insufficient Ni supplied in Cu_6Sn_5 to fully stabilise the hexagonal phase when the hexagonal-monoclinic transformation is driven by ageing.

The sustainability of the stabilisation effect brought by Ni/Zn during the ageing process needs further investigation. Moreover $(Cu,Au,Ni)_6Sn_5$ stabilisation also needs to be compared to that of $(Cu,Ni)_6(Sn,Zn)_5$, under conditions of both reflow and aged. Synchrotron XRD patterns in Fig.9 provide a comprehensive/direct comparison on the phase stability of interfacial Cu_6Sn_5 intermetallic, as influenced by ageing and alloying composition variations. Firstly, it is noted that interfacial $(Cu,Au)_6Sn_5$ was stabilised and remained hexagonal after reflow. The phase stability of interfacial Cu_6Sn_5 intermetallic in BGA solder joints obviously degraded with the process of ageing at 150℃. Pure Cu_6Sn_5 (without alloying elements) experienced a solid-state polymorphic (metastable hexagonal to monoclinic) phase transformation during ageing. In Sn-0.7Cu/Cu, additional peaks indexed as the monoclinic phase (as indicated by arrows) are gradually discernable from 0h to 1,500h ageing.

It should be emphasised that alloying elements Ni/Au/Zn into Sn-0.7Cu were able to decelerate the progress of this phase transformation. Although, the ability of delaying this phase transformation among these alloying elements differs. In Sn-0.7Cu-0.4Zn-0.03Ni/Cu after 500h ageing, Cu_6Sn_5 remained as hexagonal phase

and no monoclinic phase was found. The fraction of monoclinic phase remained minimal after 1500h, indicating that the interfacial layer mainly remained as hexagonal $(Cu,Ni)_6(Sn,Zn)_5$. In contrast, the stabilising effect of Au (Sn-0.7Cu-0.06Au-0.05Ni/Cu and Sn-0.7Cu-0.06Au/Cu) is not as strong as the effect brought on by adding 0.4wt.% Zn showing in both Sn-0.7Cu-0.4Zn/Cu and Sn-0.7Cu-0.4Zn-0.03Ni/Cu, and just slightly stronger than $(Cu,Ni)_6(Sn,Zn)_5$ in Sn-0.7Cu-0.06Zn-0.05Ni/Cu. This can be rationalised with reference to distribution of alloying elements in Fig.8, where Ni remained in the growing Cu_3Sn and Au was still relatively homogeneously distributed within Cu_6Sn_5. Consequently, the phase largely became $(Cu,Au)_6Sn_5$ and only trace Au was responsible for stabilising the Cu_6Sn_5. In summary, the ageing process would compromise the phase stability of Cu_6Sn_5, whereas alloyed Cu_6Sn_5 would delay the hexagonal-monoclinic transformation and improve the stability. This stabilisation effect on hexagonal Cu_6Sn_5 was also found to be sensitive to the amount of alloying elements doped within the Cu_6Sn_5.

Overall, Ni and Zn concurrent additions seem to have most significant stabilising effects on Sn-0.7Cu/Cu solder joints among these candidates. The stabilisation effects includes refinement of the microstructure[1], domination of $(Cu,Ni)_6Sn_5$ and suppression of the growth of Cu_3Sn in the interfacial layer[1] and inhibiting the polymorphic phase transformation of Cu_6Sn_5[34, 35], as well as minimising the thermal expansion mismatch between interfacial Cu_6Sn_5 and the Cu substrate[1]. This is explained by the fact that Ni and Zn additions alter the solidification path of Sn-0.7Cu solder alloys and lead to a more thermodynamically stable Cu_6Sn_5. The present study has shown for the first time, that micro-alloying Ni/Zn stabilisation effects can remain effective even after 1500h ageing.

3.4 Effect of Au on the thermal expansion behaviour of $(Cu,Au)_6Sn_5$ and $(Cu,Au,Ni)_6Sn_5$.

We have previously discussed how the Ni/Zn stabilising effect minimises the thermal expansion mismatch between interfacial Cu_6Sn_5 and the Cu substrate [1]. It was of great interest in this study to compare the influence of Au alloying, on the minimisation of thermal expansion mismatch to that of Zn alloying. In-situ XRD patterns of Sn-0.7Cu-0.06Au/Cu and Sn-0.7Cu-0.06Au-0.05Ni/Cu were measured in the range of 30℃-250℃ (Appendix B). The complete indexing of peaks of the patterns performed by Le-Bail fitting can be found in Appendix A. It clearly shows that 2θ of peaks shifted towards a lower angle as the temperature increased. But qualitatively the shift extent of each peak varied, which indicated the anisotropic behaviour in thermal expansion of the intermetallics. This can be quantified by the change in the c/a ratio of Cu_6Sn_5 crystals with whole pattern fitting. Fig.10 (a-c) shows the relative change in lattice parameters and cell volume of Cu_6Sn_5 (with/without alloying) with temperature. Discontinuity in expansion in the temperature range of 180-210℃, was caused by a polymorphic phase transformation of Cu_6Sn_5[1]. It was noted that Au (when it is solely added into Sn-0.7Cu with the composition of Sn-0.7Cu-0.06Au) had an impact on reducing the Cu_6Sn_5/Cu thermal expansion mismatch and also resulted in slightly isotropic thermal expansion behavior. However, it was surprising in Fig.10b and c that concurrent Ni and Au alloying in a Sn-0.7Cu-0.06Au-0.05Ni/Cu couple exhibited a similar behavior to that of Sn-0.7Cu/Cu and was not beneficial in terms of reducing the expansion mismatch.

4. Conclusions

Based on the previous findings, this study was performed to explore the influence of ageing on the phase stability of interfacial $(Cu,Ni)_6(Sn,Zn)_5$ and $(Cu,Au,Ni)_6Sn_5$ intermetallic in Pb-free BGA joints. The following conclusions can be made;

1) Alloying elements influenced the thickness ratio of the interfacial Cu_6Sn_5/Cu_3Sn layers during aging. Unlike Zn microalloying, 0.06wt.%Au was not able to suppress interfacial Cu_3Sn growth in Sn-0.7Cu-0.06Au/Cu and also hindered the Ni suppression effect in Sn-0.7Cu-0.06Au-0.05Ni/Cu.

2) Ni and Au co-existed and were relatively homogeneously distributed in the interfacial Cu_6Sn_5 layer after reflow in Sn-0.7Cu-0.06Au-0.05Ni/Cu. With the progress of ageing, Cu_3Sn grew substantially and Ni was mainly located in Cu_3Sn at the interface. Au remained homogeneously distributed in the newly grown Cu_6Sn_5, which was in contrast to the Sn-0.7Cu-0.4Zn-0.05Ni/Cu system[1].

3) Interfacial hexagonal Cu_6Sn_5 phase continuously transformed to monoclinic Cu_6Sn_5 with the progress of solid-state ageing at 150℃. Alloying Ni/Zn/Au, especially with 0.4 wt.% Zn into Sn-0.7Cu, decelerated this progress and phase stability of interfacial Cu_6Sn_5 was improved, compared to Cu_6Sn_5 in the Sn-0.7Cu/Cu system.

4) On ageing, Au stabilising effects on $(Cu,Au,Ni)_6Sn_5$ by 0.06wt.%Au and 0.05wt.%Ni additions was still slightly stronger than $(Cu,Ni)_6(Sn,Zn)_5$ in Sn-0.7Cu-0.06Zn-0.05Ni/Cu.

5) 0.06wt.%Au addition into Sn-0.7Cu had an impact on reducing the Cu_6Sn_5/Cu thermal expansion mismatch, but not in the case of concurrent additions of Ni and Au in Sn-0.7Cu-0.06Au-0.05Ni/Cu.

Acknowledgements

We gratefully acknowledge financial support from the University of Queensland-Nihon Superior collaborative research program. Synchrotron micro XRF mapping was performed at the Japan Synchrotron Radiation Research Institute (JASRI) on BL37XU of the SPring-8 synchrotron, under Proposal No. 2012B1440 and 2013B1524, partially funded by the Australian Synchrotron international synchrotron access program (AS/IA124/6235). PXRD experiments were performed at the Australian Synchrotron Powder Diffraction Beamline (AS132/PD/5784). This work is also supported in part by a Grant-in-Aid for Scientific Research (A) (24246124) from JSPS, Japan. The authors acknowledge the facilities, and the scientific and technical assistance, of the Australian Microscopy & Microanalysis Research Facility at the Centre for Microscopy and Microanalysis of UQ. The authors thank Mr. Jonathan Read of the University of Queensland for valuable discussions. G. Zeng gratefully thanks for Dr. Mark D Callaghan of the University of Manchester, UK for manuscript editing. G. Zeng acknowledges the financial support of a University of Queensland International (UQI) Scholarship, a Graduate School International Travel Award (GSITA) of UQ, and the China Scholarship Council (CSC).

References

[1] G. Zeng, S.D. McDonald, Q. Gu, Y. Terada, K. Uesugi, H. Yasuda, K. Nogita, The influence of Ni

and Zn additions on microstructure and phase transformations in Sn–0.7 Cu/Cu solder joints, Acta Mater. 83 (2015) 357-371.

[2] A.A. El-Daly, H. El-Hosainy, T.A. Elmosalami, W.M. Desoky, Microstructural modifications and properties of low-Ag-content Sn–Ag–Cu solder joints induced by Zn alloying, J. Alloys Compd. 653 (2015) 402-410.

[3] J. Koo, C. Lee, S.J. Hong, K.-S. Kim, H.M. Lee, Microstructural discovery of Al addition on Sn–0.5Cu-based Pb-free solder design, J. Alloys Compd. 650 (2015) 106-115.

[4] Z.L. Ma, S.A. Belyakov, C.M. Gourlay, Effects of cobalt on the nucleation and grain refinement of Sn-3Ag-0.5Cu solders, J. Alloys Compd. 682 (2016) 326-337.

[5] M. Yang, H. Ji, S. Wang, Y.-H. Ko, C.-W. Lee, J. Wu, M. Li, Effects of Ag content on the interfacial reactions between liquid Sn–Ag–Cu solders and Cu substrates during soldering, J. Alloys Compd. 679 (2016) 18-25.

[6] J.W. Xian, S.A. Belyakov, C.M. Gourlay, Controlling Bulk Cu_6Sn_5 Nucleation in Sn0.7Cu/Cu Joints with Al Micro-alloying, J. Electron. Mater. 45 (2016) 69-78.

[7] T. Laurila, V. Vuorinen, M. Paulasto-Kröckel, Impurity and alloying effects on interfacial reaction layers in Pb-free soldering, Mater. Sci. Eng., R 68 (2010) 1-38.

[8] K. Nogita, D. Mu, S.D. McDonald, J. Read, Y.Q. Wu, Effect of Ni on phase stability and thermal expansion of $Cu_{6-x}Ni_xSn_5$ (X = 0, 0.5, 1, 1.5 and 2), Intermetallics 26 (2012) 78-85.

[9] C.M. Gourlay, K. Nogita, A.K. Dahle, Y. Yamamoto, K. Uesugi, T. Nagira, M. Yoshiya, H. Yasuda, In situ investigation of unidirectional solidification in Sn–0.7Cu and Sn–0.7Cu–0.06Ni, Acta Mater. 59 (2011) 4043-4054.

[10] K. Nogita, T. Nishimura, Nickel-stabilized hexagonal $(Cu,Ni)_6Sn_5$ in Sn–Cu–Ni lead-free solder alloys, Scripta Mater. 59 (2008) 191-194.

[11] R. Gagliano, G. Ghosh, M. Fine, Nucleation kinetics of Cu_6Sn_5 by reaction of molten tin with a copper substrate, J. Electron. Mater. 31 (2002) 1195-1202.

[12] G. Ghosh, M. Asta, Phase stability, phase transformations, and elastic properties of Cu_6Sn_5: Ab initio calculations and experimental results, J. Mater. Res. 20 (2005) 3102-3117.

[13] Y.Q. Wu, S.D. McDonald, J. Read, H. Huang, K. Nogita, Determination of the minimum Ni concentration to prevent the η to η^{4+1} polymorphic transformation of stoichiometric Cu_6Sn_5, Scripta Mater. 68 (2013) 595-598.

[14] K. Nogita, Stabilisation of Cu_6Sn_5 by Ni in Sn-0.7Cu-0.05Ni lead-free solder alloys, Intermetallics 18 (2010) 145-149.

[15] C.M. Gourlay, J. Read, K. Nogita, A.K. Dahle, The maximum fluidity length of solidifying Sn-Cu-Ag-Ni solder alloys, J. Electron. Mater. 37 (2008) 51-60.

[16] T. Ventura, S. Terzi, M. Rappaz, A.K. Dahle, Effects of Ni additions, trace elements and solidification kinetics on microstructure formation in Sn–0.7Cu solder, Acta Mater. 59 (2011) 4197-4206.

[17] T. Ventura, Y.-H. Cho, C. Kong, A.K. Dahle, Formation of Intermetallics in Sn-0.9 Cu and Sn-0.7 Cu-0.08 Ni Solders, J. Electron. Mater. 40 (2011) 1403-1408.

[18] C.M. Gourlay, K. Nogita, S.D. McDonald, T. Nishimura, K. Sweatman, A.K. Dahle, A rheological assessment of the effect of trace level Ni additions on the solidification of Sn–0.7Cu, Scripta Mater. 54 (2006) 1557-1562.

[19] H. Yu, V. Vuorinen, J. Kivilahti, Effect of Ni on the formation of Cu_6Sn_5 and Cu_3Sn intermetallics, IEEE T. Electron. Pack. 30 (2007) 293-298.

[20] G. Zeng, S.D. McDonald, D. Mu, Y. Terada, H. Yasuda, Q. Gu, K. Nogita, Ni segregation in the interfacial $(Cu,Ni)_6Sn_5$ intermetallic layer of Sn-0.7 Cu-0.05 Ni/Cu ball grid array (BGA) joints, Intermetallics 54 (2014) 20-27.

[21] M.J. Rizvi, C. Bailey, Y.C. Chan, H. Lu, Effect of adding 0.3 wt% Ni into the Sn-0.7 wt%Cu solder. Part I: Wetting behavior on Cu and Ni substrates, J. Alloys Compd. 438 (2007) 116-121.

[22] D. Mu, H. Yasuda, H. Huang, K. Nogita, Growth orientations and mechanical properties of Cu_6Sn_5 and $(Cu,Ni)_6Sn_5$ on poly-crystalline Cu, J. Alloys Compd. 536 (2012) 38-46.

[23] H. Tsukamoto, T. Nishimura, S. Suenaga, S.D. McDonald, K.W. Sweatman, K. Nogita, The influence of solder composition on the impact strength of lead-free solder ball grid array joints, Microelectron. Reliab. 51 (2011) 657-667.

[24] D. Swenson, The effects of suppressed beta tin nucleation on the microstructural evolution of lead-free solder joints, J. Mater. Sci. - Mater. Electron. 18 (2007) 39-54.

[25] G. Zeng, S.D. McDonald, C.M. Gourlay, K. Uesugi, Y. Terada, H. Yasuda, K. Nogita, Solidification of Sn-0.7 Cu-0.15 Zn Solder: In Situ Observation, Metall. Mater. Trans. A 45 (2014) 918-926.

[26] S.H. Huh, K.S. Kim, K. Suganuma, Effect of Au addition on microstructural and mechanical properties of Sn-Cu eutectic solder, Mater. Trans., JIM 43 (2002) 239-245.

[27] S.A. Belyakov, C.M. Gourlay, Heterogeneous nucleation of βSn on $NiSn_4$, $PdSn_4$ and $PtSn_4$, Acta Mater. 71 (2014) 56-68.

[28] A. Gangulee, G.C. Das, M.B. Bever, An x-ray diffraction and calorimetric investigation of the compound Cu_6Sn_5, Metall. Mater. Trans. B 4 (1973) 2063-2066.

[29] K. Nogita, C.M. Gourlay, S.D. McDonald, Y.Q. Wu, J. Read, Q.F. Gu, Kinetics of the η-η' transformation in Cu_6Sn_5, Scripta Mater. 65 (2011) 922-925.

[30] C. Yu, J. Liu, H. Lu, P. Li, J. Chen, First-principles investigation of the structural and electronic properties of Cu6−xNixSn5 (x=0, 1, 2) intermetallic compounds, Intermetallics 15 (2007) 1471-1478.

[31] B. Peplinski, G. Schulz, D. Schultze, E. Schierhorn, Improved X-Ray Powder Diffraction Data for the Disordered η-Cu_6Sn_5 Alloy Phase, Mater. Sci. Forum 228 (1996) 577-582.

[32] A.K. Larsson, L. Stenberg, S. Lidin, The superstructure of domain-twinned eta'-Cu_6Sn_5, Acta Crystallogr. Sect. B: Struct. Sci. 50 (1994) 636-643.

[33] Y. Watanabe, Y. Fujinaga, H. Iwasaki, Lattice modulation in the long-period superstructure of Cu_3Sn, Acta Crystallogr. Sect. B: Struct. Sci. 39 (1983) 306-311.

[34] G. Zeng, S.D. McDonald, Q. Gu, K. Nogita, Effect of Zn, Au, and In on the polymorphic phase transformation in Cu_6Sn_5 intermetallics, J. Mater. Res. 27 (2012) 2609-2614.

[35] G. Zeng, S.D. McDonald, Q. Gu, S. Suenaga, Y. Zhang, J. Chen, K. Nogita, Phase stability and

thermal expansion behavior of Cu_6Sn_5 intermetallics doped with Zn, Au and In, Intermetallics 43 (2013) 85-98.

[36] Y. Terada, H. Yumoto, A. Takeuchi, Y. Suzuki, K. Yamauchi, T. Uruga, New X-ray microprobe system for trace heavy element analysis using ultraprecise X-ray mirror optics of long working distance, Nucl. Instrum. Methods Phys. Res., Sect. A 616 (2010) 270-272.

[37] K.S. Wallwork, B.J. Kennedy, D. Wang, The High Resolution Powder Diffraction Beamline for the Australian Synchrotron, AIP Conference Proceedings 879 (2007) 879-882.

[38] M.R. Rowles, I.C. Madsen, Whole-pattern profile fitting of powder diffraction data collected in parallel-beam flat-plate asymmetric reflection geometry, J. Appl. Crystallogr. 43 (2010) 632-634.

[39] B.L. Henke, E.M. Gullikson, J.C. Davis, X-Ray Interactions: Photoabsorption, Scattering, Transmission, and Reflection at E= 50-30,000 eV, Z= 1-92, At. Data Nucl. Data Tables 54 (1993) 181-342.

[40] R. Labie, W. Ruythooren, J. Van Humbeeck, Solid state diffusion in Cu–Sn and Ni–Sn diffusion couples with flip-chip scale dimensions, Intermetallics 15 (2007) 396-403.

[41] J. Gong, C. Liu, P.P. Conway, V.V. Silberschmidt, Evolution of CuSn intermetallics between molten SnAgCu solder and Cu substrate, Acta Mater. 56 (2008) 4291-4297.

[42] M.A.A. Mohd Salleh, S.D. McDonald, H. Yasuda, A. Sugiyama, K. Nogita, Rapid Cu6Sn5 growth at liquid Sn/solid Cu interfaces, Scripta Mater. 100 (2015) 17-20.

[43] M.S. Park, R. Arróyave, Concurrent nucleation, formation and growth of two intermetallic compounds (Cu_6Sn_5 and Cu_3Sn) during the early stages of lead-free soldering, Acta Mater. 60 (2012) 923-934.

[44] K.N. Tu, R.D. Thompson, Kinetics of interfacial reaction in bimetallic Cu-Sn thin films, Acta Metall. 30 (1982) 947-952.

[45] C. Yu, D. Wang, J. Chen, J. Xu, J. Chen, H. Lu, Study of Cu_6Sn5 and Cu_3Sn growth behaviors by considering trace Zn, Mater. Lett. 121 (2014) 166-169.

[46] Y.W. Wang, C.C. Chang, C.R. Kao, Minimum effective Ni addition to SnAgCu solders for retarding Cu_3Sn growth, J. Alloys Compd. 478 (2009) L1-L4.

[47] C.-Y. Yu, W.-Y. Chen, J.-G. Duh, Suppressing the growth of Cu–Sn intermetallic compounds in Ni/Sn–Ag–Cu/Cu–Zn solder joints during thermal aging, Intermetallics 26 (2012) 11-17.

[48] Y.W. Wang, Y.W. Lin, C.T. Tu, C.R. Kao, Effects of minor Fe, Co, and Ni additions on the reaction between SnAgCu solder and Cu, J. Alloys Compd. 478 (2009) 121-127.

[49] V. Vuorinen, H. Yu, T. Laurila, J.K. Kivilahti, Formation of intermetallic compounds between liquid Sn and various $CuNi_x$ metallizations, J. Electron. Mater. 37 (2008) 792-805.

[50] T. Laurila, V. Vuorinen, J.K. Kivilahti, Interfacial reactions between lead-free solders and common base materials, Mater. Sci. Eng., R 49 (2005) 1-60.

[51] V. Vuorinen, T. Laurila, T. Mattila, E. Heikinheimo, J.K. Kivilahti, Solid-state reactions between Cu (Ni) alloys and Sn, J. Electron. Mater. 36 (2007) 1355-1362.

[52] T. Laurila, A. Paul, IEEE, 2014, pp. 1-8.

[53] V.A. Baheti, S. Islam, P. Kumar, R. Ravi, R. Narayanan, D. Hongqun, V. Vuorinen, T. Laurila, A.

Paul, Effect of Ni content on the diffusion-controlled growth of the product phases in the Cu (Ni)–Sn system, Philos. Mag. 96 (2016) 15-30.

[54] G. Ross, V. Vuorinen, M. Paulasto-Kröckel, Void formation and its impact on Cu-Sn intermetallic compound formation, J. Alloys Compd. (2016).

[55] H. Yu, V. Vuorinen, J.K. Kivilahti, Solder/substrate interfacial reactions in the Sn-Cu-Ni interconnection system, J. Electron. Mater. 36 (2007) 136-146.

[56] B. Chao, S.-H. Chae, X. Zhang, K.-H. Lu, J. Im, P.S. Ho, Investigation of diffusion and electromigration parameters for Cu–Sn intermetallic compounds in Pb-free solders using simulated annealing, Acta Mater. 55 (2007) 2805-2814.

[57] K. Tu, Interdiffusion and reaction in bimetallic Cu-Sn thin films, Acta Metall. 21 (1973) 347-354.

[58] K.C. Huang, F.S. Shieu, Y.H. Hsiao, C.Y. Liu, Ni Interdiffusion Coefficient and Activation Energy in Cu_6Sn_5, J. Electron. Mater. 41 (2012) 172-175.

[59] C. Chang, Q. Lee, C. Ho, C. Kao, Cross-interaction between Au and Cu in Au/Sn/Cu ternary diffusion couples, J. Electron. Mater. 35 (2006) 366-371.

[60] Y.-W. Yen, H. Tseng, K. Zeng, S. Wang, C. Liu, Cross-interaction between Au/Sn and Cu/Sn interfacial reactions, J. Electron. Mater. 38 (2009) 2257-2263.

[61] C.F. Yang, S.W. Chen, Interfacial reactions in Au/Sn/Cu sandwich specimens, Intermetallics 18 (2010) 672-678.

[62] J. Farjas, P. Roura, Modification of the Kolmogorov–Johnson–Mehl–Avrami rate equation for non-isothermal experiments and its analytical solution, Acta Mater. 54 (2006) 5573-5579.

[63] G. Zeng, S.D. McDonald, J.J. Read, Q. Gu, K. Nogita, Kinetics of the polymorphic phase transformation of Cu_6Sn_5, Acta Mater. 69 (2014) 135-148.

Figure Captions

Fig.1 Experimental setup for synchrotron XRF and XRD; (a) XRF setting at BL37XU of SPring-8, (b-c) sample of cross-sectioned BGA joint sample with 100µm thickness, used for XRF; (d) glancing angle XRD in reflection mode at Powder Diffraction beamline of Australian Synchrotron, and (e-f) samples of interfacial intermetallic layer of Sn-0.7Cu-0.05Ni-0.06Zn/Cu used for XRD; (e) as-soldered and (f) after aged at 150℃ for 1500h.

Fig.2 Le-Bail fitting and indexing of interfacial Cu_6Sn_5 (hexagonal, $P6_3/mmc$) and Cu, as well as the layer of Cu_3Sn.

Fig.3 Cross-sectioned views of Sn-0.7Cu-0.4Zn-0.03Ni/Cu BGA solder joints under (a-b) as-reflowed and (c-d) 500h ageing conditions.

Fig.4 Cross-sectioned views of Sn-0.7Cu-0.06Au-0.05Ni/Cu solder joints under conditions of (a-b) as-reflowed; (c-d) 500h ageing.

Fig.5 Cross-sectioned views of interfacial intermetallic layers of BGA solder joints after annealing at 150℃ for 500 hours. Sn-0.7Cu-0. 4Zn-0.03Ni, Sn-0.7Cu-0.06Au and Sn-0.7Cu-0.06Au-0.05Ni are compared to compositions with Ni and Zn additions studied in previous work [1, 25] (Sn-0.7Cu, Sn-0.7Cu-0.05Ni, Sn-0.7Cu-0.15Zn and Sn-0.7Cu-0.06Zn-0.03Ni).

Fig.6 Synchrotron XRF mapping of interfacial $(Cu,Ni)_6(Sn,Zn)_5$ intermetallic layers of as-reflowed Sn-0.7Cu-0.06Zn-0.05Ni/Cu BGA solder joint (Exposure time: 0.3 s, scan pitch is 100 nm).

Fig.7 Synchrotron XRF mapping of interfacial $(Cu,Ni,Au)_6Sn_5$ intermetallic layers of as-soldered Sn-0.7Cu-0.05Ni-0.06Au/Cu BGA solder joint (Exposure time: 0.3 s, scan pitch is 100 nm).

Fig.8 Synchrotron XRF mapping of interfacial $(Cu,Ni,Au)_6Sn_5$ intermetallic layers in Sn-0.7Cu-0.05Ni-0.06Au/Cu BGA solder joint after 500h ageing (Exposure time: 0.3 s, scan pitch is 200 nm, arrow is used for location reference).

Fig.9 Glancing angle synchrotron XRD diffraction of interfacial intermetallic layer of BGA solder joints (a) as-soldered, (b) after 500h ageing and (c) after 1500h ageing.

Fig.10 Thermal expansion behaviour of interfacial Cu_6Sn_5 and Cu substrate Cu in the temperature range 30-250℃: (a) the variation i n lattice parameters of (a) Sn-0.7Cu-0.06Au and (b) Sn-0.7Cu-0.06Au-0.05Ni compared to previous solder compositions investigated; (c) volumetric thermal expansion behaviour compared to previous solder compositions investigated, and (d) variation of c/a ratio with temperature. Thermal expansion (%) = $(a_T-a_0)/a_0 \times 100\%$ (a_0 is lattice parameter at room temperature; and a_T is lattice parameters at temperature T.)

Table Captions

Table 1 Crystal structure of Cu_6Sn_5 and Cu_3Sn phases

Phase	Space group	Formula	Prototype	System	Pearson Symbol	Lattice parameters	Stable Temperature range	Reference
η' Cu_6Sn_5	C 1 2/c 1	Cu_6Sn_5	Cu_5Sn_5	Monoclinic	mS44	a=11.022(5) b=7.282(4) c=9.827(2) β=98.84(4)	< 186℃	[41]
η Cu_6Sn_5	P 63/m m c	Cu_6Sn_5 (CuSn)	NiAs	Hexagonal	hP4	a=4.1980 c=5.0960	>186℃ or >210℃	[35]
η $^{4+1}$ Cu_6Sn_5	P 1	$Cu_{46}Sn_{37}$	\	Triclinic	aP332	a=92.2410(8) b=7.31077(7) c=9.879989 β=118.952	<210℃	[5]
ε Cu_3Sn	C m c m	$Cu_{3.02}Sn_{0.98}$	\	Orthorhombic	oS80	5.529(8) 47.75(6) 4.323(5)	\	[42]

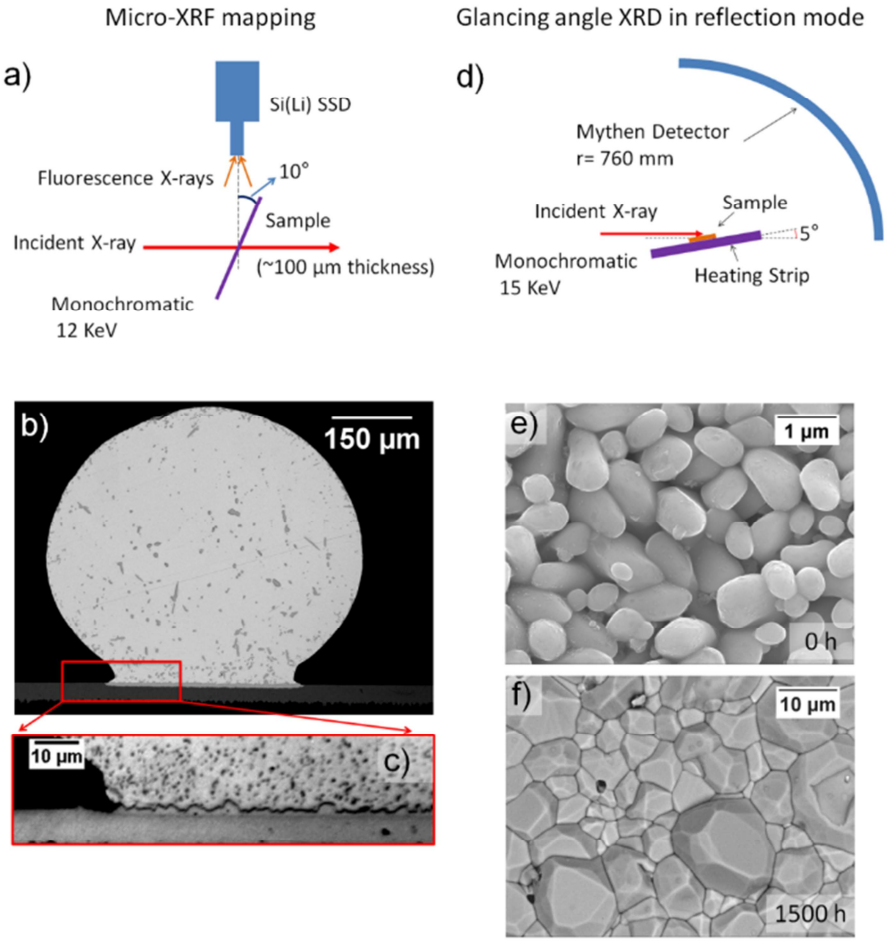

Fig.1 Experimental setup for synchrotron XRF and XRD; (a) XRF setting at BL37XU of SPring-8, (b-c) sample of cross-sectioned BGA joint sample with 100µm thickness, used for XRF; (d) glancing angle XRD in reflection mode at Powder Diffraction beamline of Australian Synchrotron, and (e-f) samples of interfacial intermetallic layer of Sn-0.7Cu-0.05Ni-0.06Zn/Cu used for XRD; (e) as-soldered and (f) after being aged at 150℃ for 1500h.

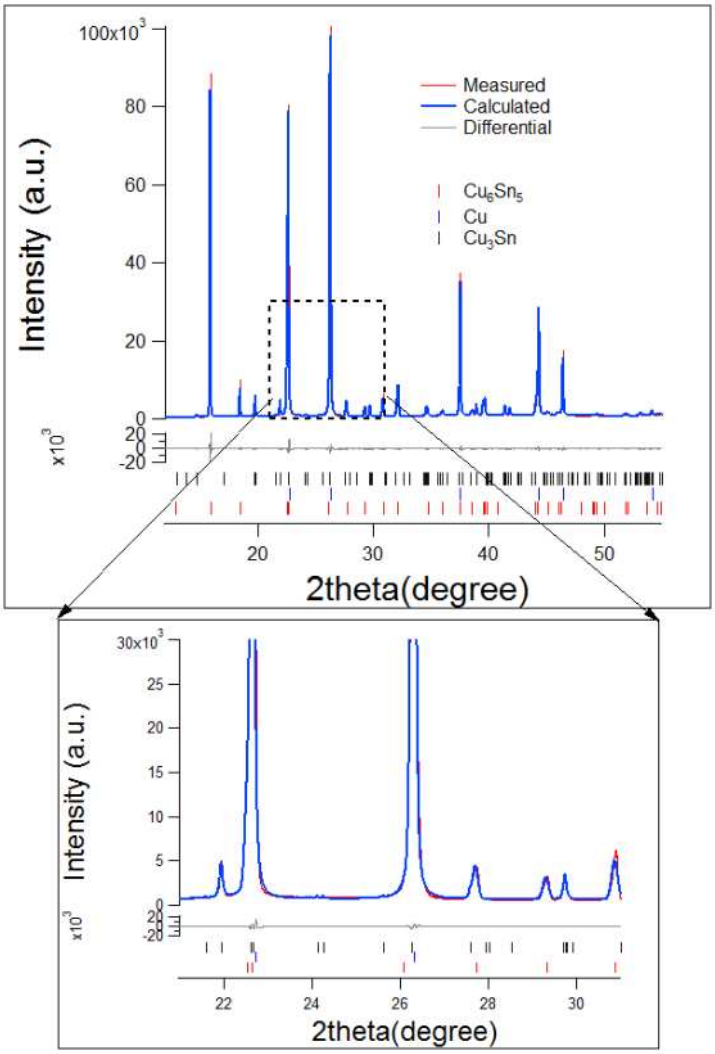

Fig.2 Le-Bail fitting and indexing of interfacial Cu_6Sn_5 (hexagonal, $P6_3/mmc$) and Cu, as well as the layer of Cu_3Sn.

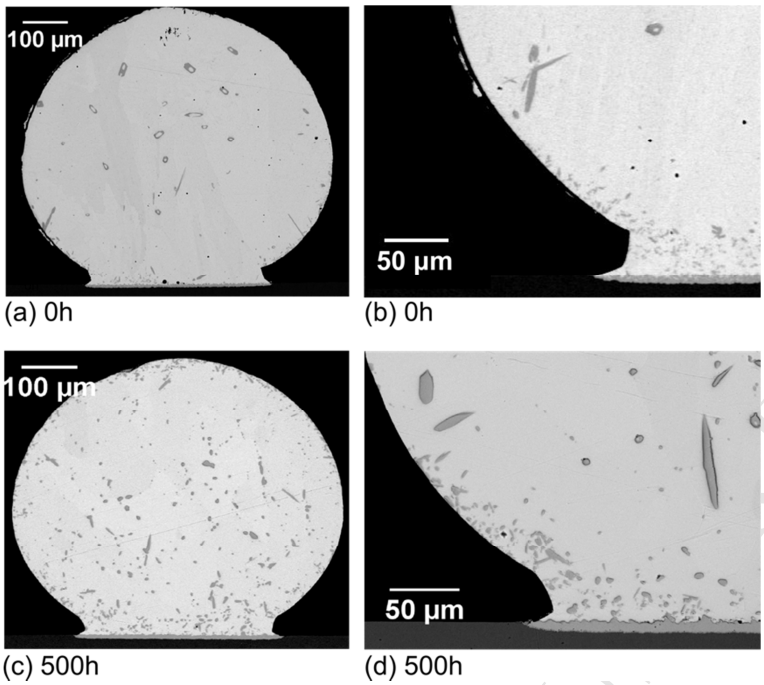

Fig.3 Cross-sectioned views of Sn-0.7Cu-0.4Zn-0.03Ni/Cu BGA solder joints under (a-b) as-reflowed; (c-d) 500h ageing;

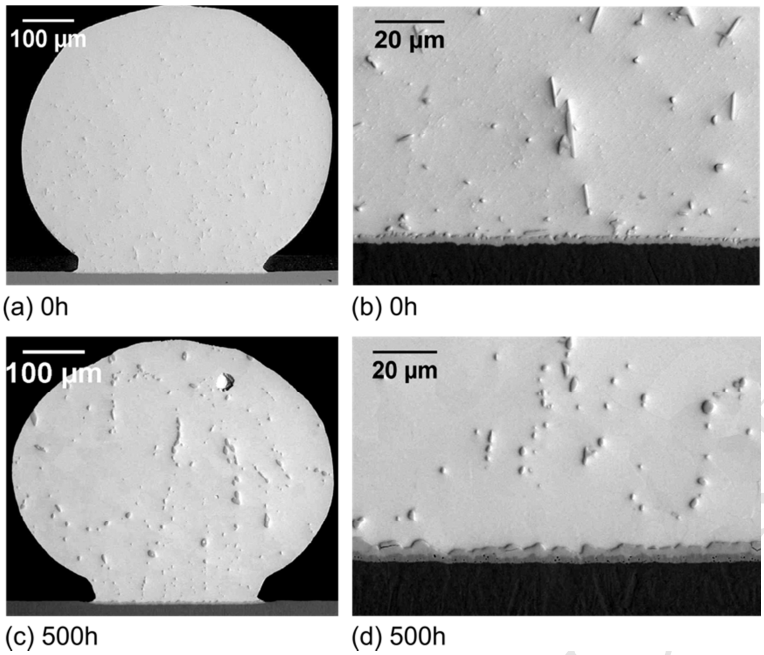

Fig.4 Cross-sectioned views of Sn-0.7Cu-0.06Au-0.05Ni/Cu solder joints under conditions of (a-b) as-reflowed; (c-d) 500h ageing.

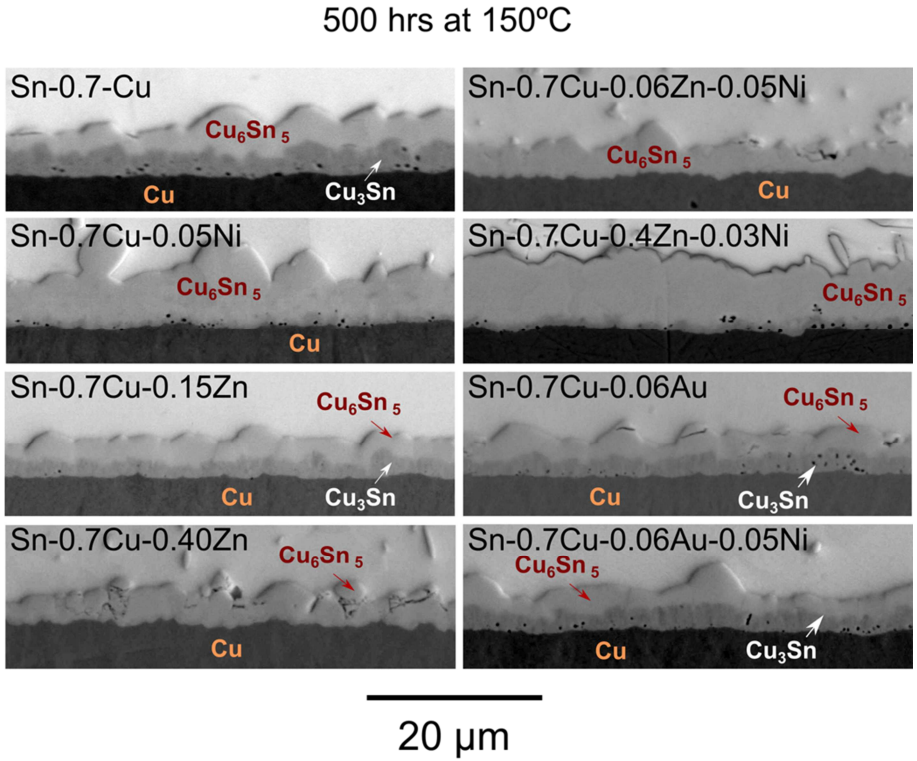

Fig.5 Cross-sectioned views of interfacial intermetallic layers of BGA solder joints after annealing at 150℃ for 500 hours. Sn-0.7Cu-0.4Zn-0.03Ni, Sn-0.7Cu-0.06Au and Sn-0.7Cu-0.06Au-0.05Ni are compared to compositions with Ni and Zn additions studied in previous work [1, 25] (Sn-0.7Cu, Sn-0.7Cu-0.05Ni, Sn-0.7Cu-0.15Zn and Sn-0.7Cu-0.06Zn-0.03Ni).

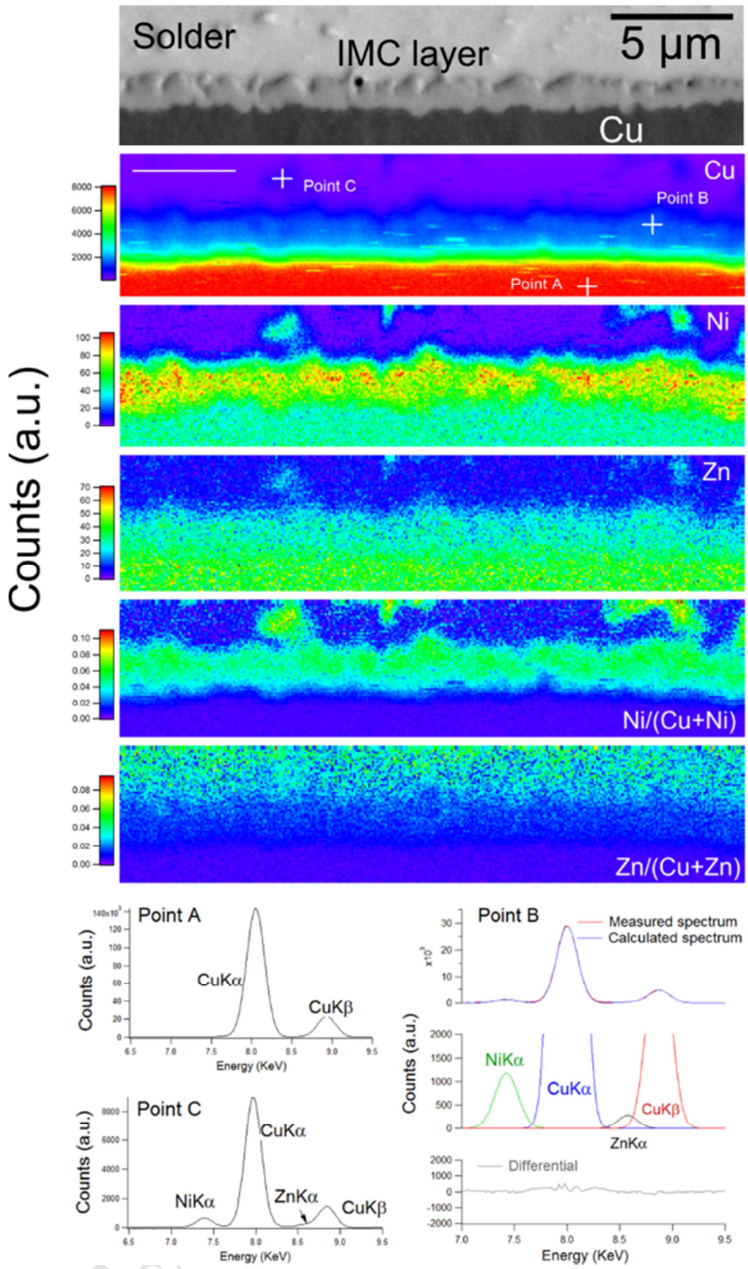

Fig.6 Synchrotron XRF mapping of interfacial $(Cu,Ni)_6(Sn,Zn)_5$ intermetallic layers of an as-reflowed Sn-0.7Cu-0.06Zn-0.05Ni/Cu BGA solder joint (Exposure time: 0.3 s, scan pitch is 100 nm).

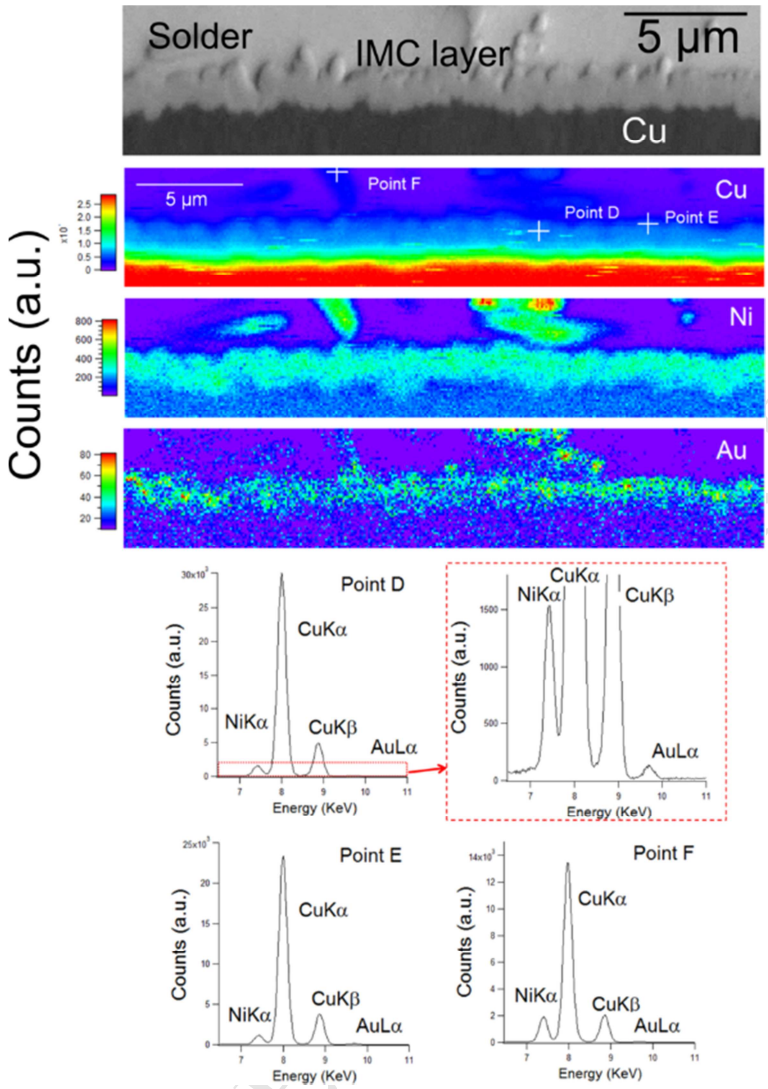

Fig.7 Synchrotron XRF mapping of interfacial $(Cu,Ni,Au)_6Sn_5$ intermetallic layers of as-soldered Sn-0.7Cu-0.05Ni-0.06Au/Cu BGA solder joint (Exposure time: 0.3 s, scan pitch is 100 nm).

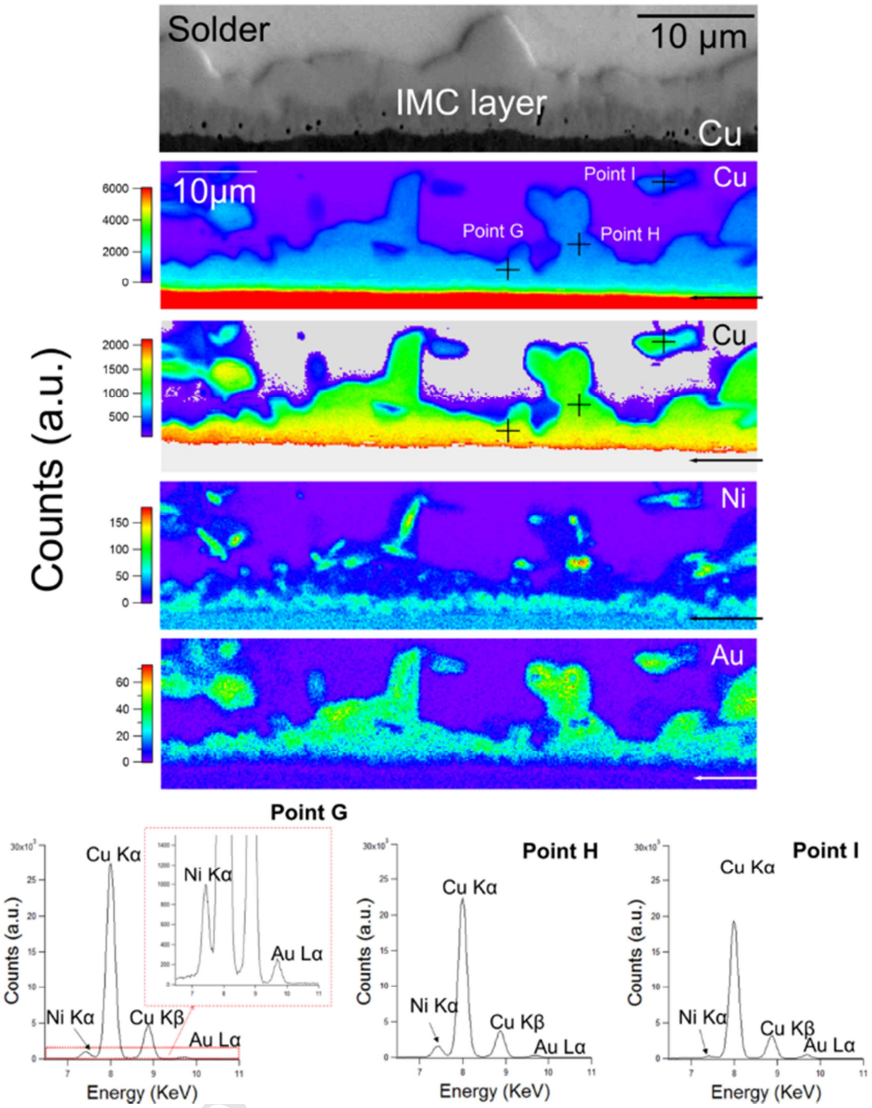

Fig.8 Synchrotron XRF mapping of interfacial $(Cu,Ni,Au)_6Sn_5$ intermetallic layers in Sn-0.7Cu-0.05Ni-0.06Au/Cu BGA solder joint after 500h ageing (Exposure time: 0.3 s, scan pitch is 200 nm, arrow is used for location reference).

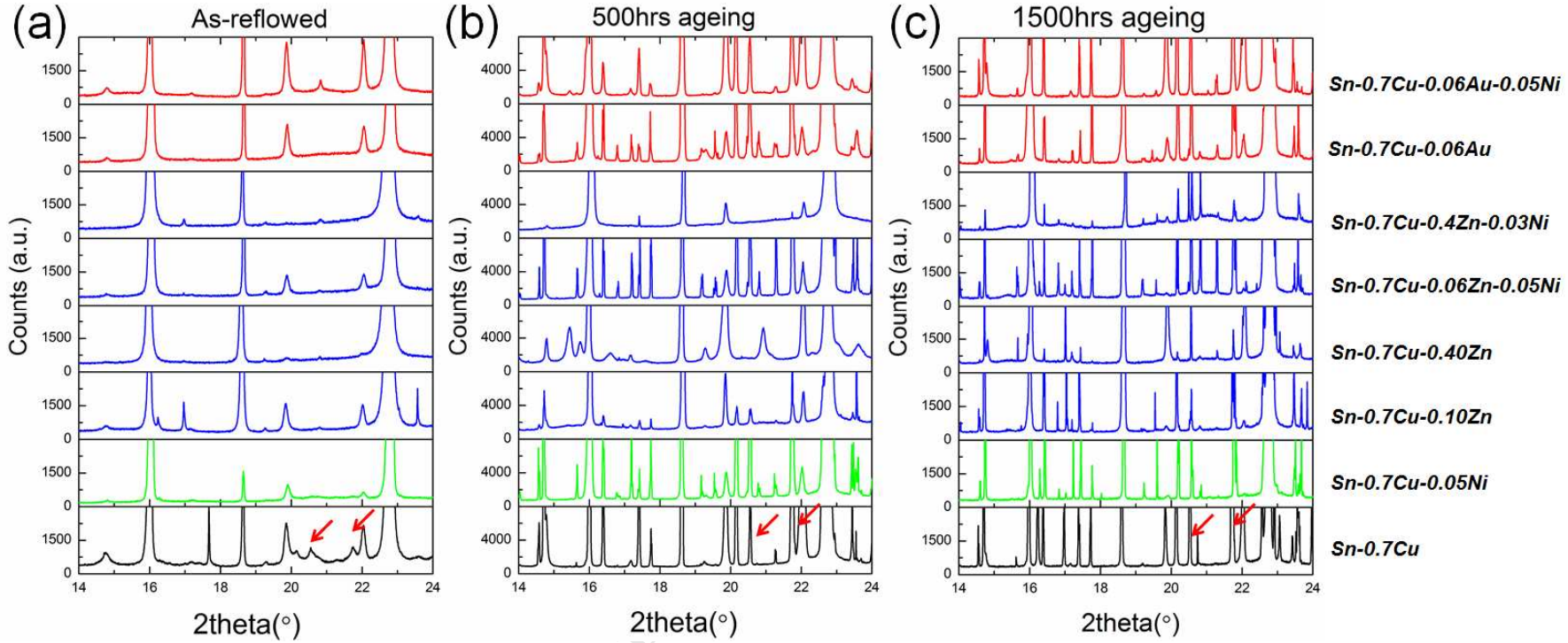

Fig.9 Glancing angle synchrotron XRD diffraction of interfacial intermetallic layer of BGA solder joints (a) as-soldered, (b) after 500h ageing and (c) after 1500h ageing.

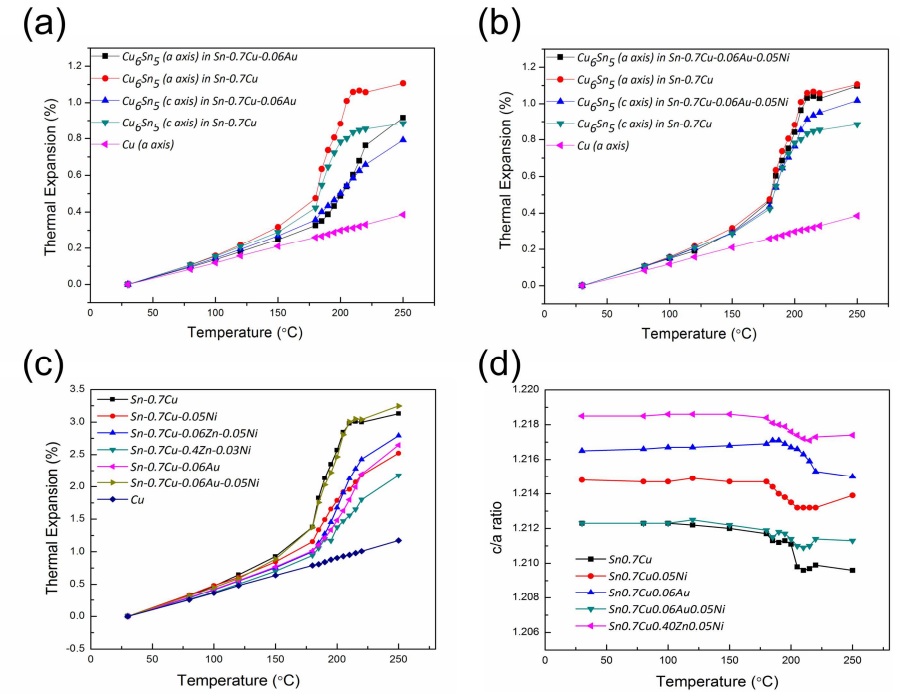

Fig.10 Thermal expansion behaviour of interfacial Cu_6Sn_5 and Cu substrate Cu in the temperature range 30-250℃: (a) the variation in la ttice parameters of (a) Sn-0.7Cu-0.06Au and (b) Sn-0.7Cu-0.06Au-0.05Ni compared to previous solder compositions investigated; (c) volumetric thermal expansion behaviour compared to previous solder compositions investigated, and (d) variation of c/a ratio with temperature. Thermal expansion (%) $= \frac{a_T - a_0}{a_0} \times 100\%$ (a_0 is lattice parameter at room temperature; and a_T is lattice parameters at temperature T.).

Highlights

- 0.06wt.%Au was not able to suppress interfacial Cu_3Sn growth in Sn-0.7Cu/Cu.
- Au remained homogeneously distributed in interfacial $(Cu,Au)_6Sn_5$ after 500h ageing.
- Interfacial Cu_6Sn_5 phases with a metastable hexagonal generally transform to monoclinic during ageing.
- This transformation during ageing was suppressed by Ni/Au/Zn at different levels.